

Supporting Information for the Biochemistry article entitled:

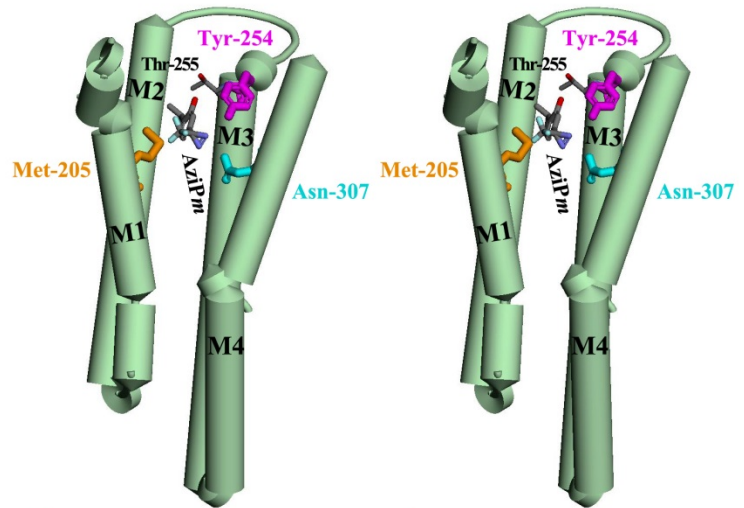
Photoaffinity Labeling the Propofol Binding Site in GLIC

by David C Chiara, Jonathan F. Gill, Qiang Chen, Tommy Tillman, William P Dailey, Roderic G. Eckenhoff, Yan Xu, Pei Tang, and Jonathan B. Cohen.

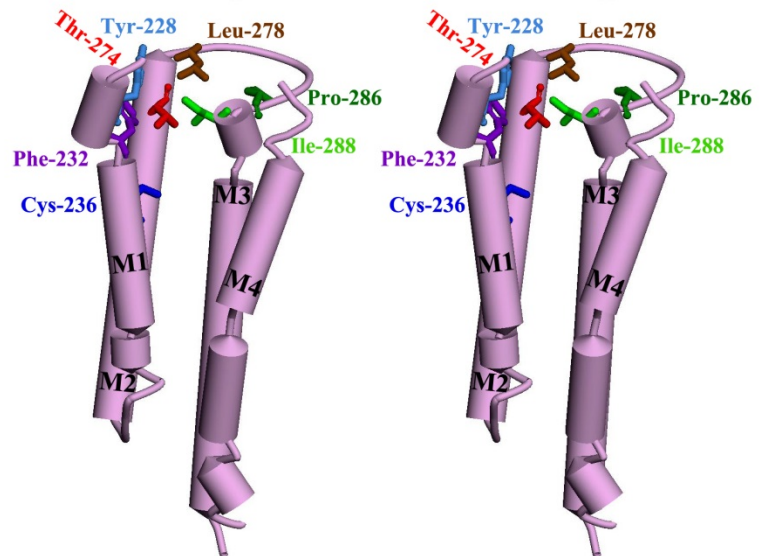
Figures S1 & S2) Stereo views of models of the transmembrane domain of pLGIC subunits, with α helices as cylinders. **A)** GLIC helix bundle pocket with AziPm (stick format, color coded by atom type: gray, carbon; red, oxygen; light blue, fluorine; blue, nitrogen) docked within the predicted propofol binding site. The 3 colored residues (Met-205, gold; Tyr-254, magenta; and Asn-307, cyan) were photolabeled by AziPm in a propofol-inhibitable manner. Also included is Thr-255, a residue that when mutated to alanine increased potency of propofol inhibition (1) but when mutated to cysteine demonstrated higher reactivity with MTSEA in the presence of propofol than in the absence (2). **B)** nAChR δ subunit from a homology model derived from the GLIC structure (PDB 3P50). **C)** δ subunit from the *Torpedo marmorata* nAChR cryoelectron microscopy structure (PDB 2BG9). Residues in the δ subunit helix bundle pocket photolabeled by nAChR inhibitors are shown in stick format, color coded to match residue labels. Color coding of residues is conserved between models B & C to highlight structural differences. Photolabeled residues include: Phe-232, Cys-236, & Thr-274 labeled by [³H]AziPm (3); Tyr-228 labeled by [¹⁴C]halothane (4); Ile-288, Phe-232, Cys-236, Thr-274, & Leu-278 labeled by 3-(trifluoromethyl)-3-(*m*-[¹²⁵I]iodophenyl)diazirine (TID) (5-7); Pro-286, Ile-288, & Phe-232 labeled by [³H]benzophenone (8); Phe-232 & Cys-236 labeled by [³H]TFD-etomidate (9); and Cys-236 labeled by [³H]azietomidate (10). The locations of residues in the M2 and M3 helices in nAChR homology model based on GLIC (**S1B** & **S2B**) are consistent with results of recent study of cross-links between substituted Cys in the nAChR α subunit M2 and M3 helices (11). The distances between the δ Phe-232, δ Thr-274, & δ Ile-288 in the two nAChR models are compared in Table S1.

Figure S1: Stereo views from the lipid of the transmembrane domain of pLGIC subunits: A) GLIC (PDB:3P50) and B & C) nAChR δ subunit from a GLIC-derived homology model (B) and the nAChR cryoelectron microscopy structure (C, PDB 2BG9).

A) GLIC subunit transmembrane domain (PDB:3P50)



B) δ subunit transmembrane domain from nAChR homology model based on GLIC (PDB:3P50)



C) δ subunit transmembrane domain from the nAChR structure (PDB:2BG9)

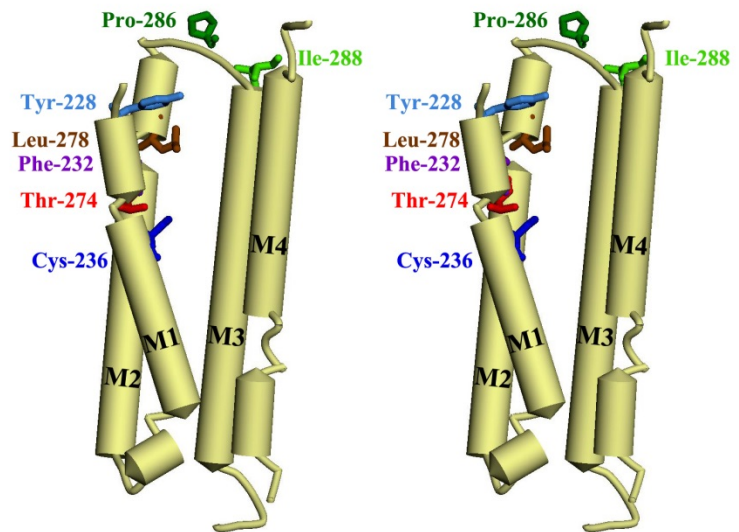


Figure S2: Stereo views from the base of the extracellular domain of the transmembrane domain of *p*LGIC subunits: A) GLIC (PDB:3P50) and B & C) nAChR δ subunit from a GLIC-derived homology model (B) and the nAChR cryoelectron microscopy structure (C, PDB 2BG9).

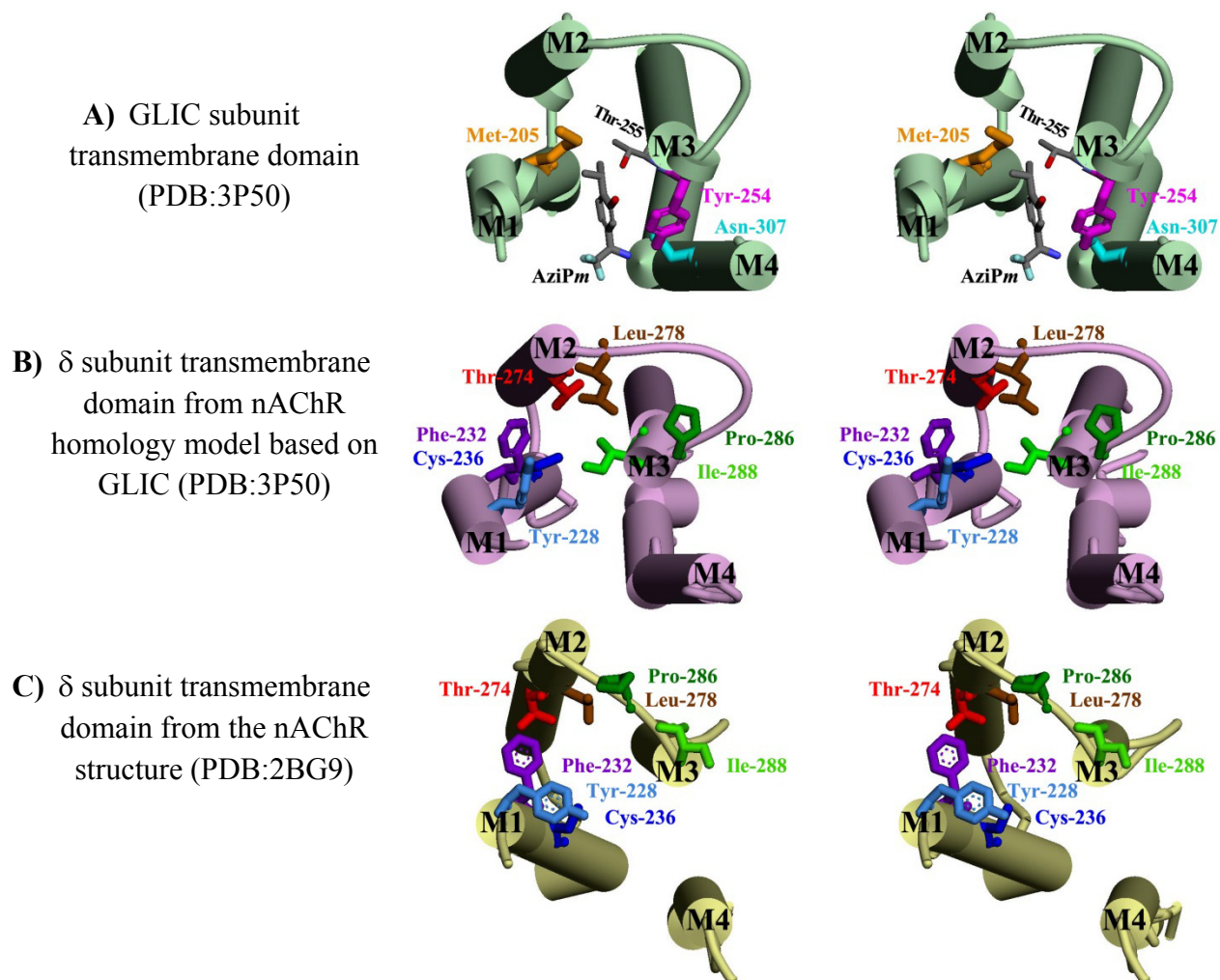


Table S1: Distances in the two nAChR models between photolabeled amino acid side chains in the δ subunit helix bundle pocket (closest non-hydrogen atoms).

	Side Chain Distances: CryoEM nAChR model (PDB:2BG9) (Å)	Side Chain Distances: nAChR homology model based on GLIC (Å)
δ Phe-232 (M1) to δ Thr-274 (M2)	5.4	3.2
δ Phe-232 (M1) to δ Ile-288 (M3)	14.3	5.9
δ Thr-274 (M2) to δ Ile-288 (M3)	17.3	4.6

References

1. Nury, H., Van Renterghem, C., Weng, Y., Tran, A., Baaden, M., Dufresne, V., Changeux, J. P., Sonner, J. M., Delarue, M., and Corringer, P. J. (2011) X-ray structures of general anaesthetics bound to a pentameric ligand-gated ion channel, *Nature* 469, 428-431.
2. Ghosh, B., Satyshur, K. A., and Czajkowski, C. (2013) Propofol Binding to the Resting State of the *Gloeobacter violaceus* Ligand-gated Ion Channel (GLIC) Induces Structural Changes in the Inter- and Intrasubunit Transmembrane Domain (TMD) Cavities, *J. Biol. Chem.* 288, 17420-17431.
3. Jayakar, S. S., Dailey, W. P., Eckenhoff, R. G., and Cohen, J. B. (2013) Identification of Propofol Binding Sites in a Nicotinic Acetylcholine Receptor with a Photoreactive Propofol Analog, *J. Biol. Chem.* 288, 6178-6189.
4. Chiara, D. C., Dangott, L. J., Eckenhoff, R. G., and Cohen, J. B. (2003) Identification of nicotinic acetylcholine receptor amino acids photolabeled by the volatile anesthetic halothane, *Biochemistry* 42, 13457-13467.
5. Arevalo, E., Chiara, D. C., Forman, S. A., Cohen, J. B., and Miller, K. W. (2005) Gating-enhanced accessibility of hydrophobic sites within the transmembrane region of the nicotinic acetylcholine receptor's δ -subunit - A time-resolved photolabeling study, *J. Biol. Chem.* 280, 13631-13640.
6. Hamouda, A. K., Chiara, D. C., Blanton, M. P., and Cohen, J. B. (2008) Probing the structure of the affinity-purified and lipid-reconstituted *Torpedo* nicotinic acetylcholine receptor, *Biochemistry* 47, 12787-12794.
7. Yamodo, I. H., Chiara, D. C., Cohen, J. B., and Miller, K. W. (2010) Conformational changes in the nicotinic acetylcholine receptor during gating and desensitization, *Biochemistry* 49, 156-165.
8. Garcia, G. III, Chiara, D. C., Nirthanan, S., Hamouda, A. K., Stewart, D. S., and Cohen, J. B. (2007) [³H]Benzophenone photolabeling identifies state-dependent changes in nicotinic acetylcholine receptor structure, *Biochemistry* 46, 10296-10307.
9. Hamouda, A. K., Stewart, D. S., Husain, S. S., and Cohen, J. B. (2011) Multiple Transmembrane Binding Sites for *p*-Trifluoromethyldiazirinyloctomidate, a Photoreactive *Torpedo* Nicotinic Acetylcholine Receptor Allosteric Inhibitor, *J. Biol. Chem.* 286, 20466-20477.
10. Chiara, D. C., Hong, F. H., Arevalo, E., Husain, S. S., Miller, K. W., Forman, S. A., and Cohen, J. B. (2009) Time-resolved photolabeling of the nicotinic acetylcholine receptor by [³H]Azietomidate, an open-state inhibitor, *Mol. Pharmacol.* 75, 1084-1095.
11. Mnatsakanyan, N. and Jansen, M. (2013) Experimental determination of the vertical alignment between the second and third transmembrane segments of muscle nicotinic acetylcholine receptors, *J. Neurochem.* 125, 843-854.